Biomedical Microdevices (2026) 28:3
https://doi.org/10.1007/s10544-025-00789-4

RESEARCH

Ultra-Sensitive and direct detection of MiRNAs in real samples via duplex-specific nuclease-mediated signal amplification

Chun-Guang Yang[1] · Yi Han[1] · Jing-Jing Zhang[2] · Li-Wen Xu[2] · Jin Li[2]

Accepted: 29 December 2025

Abstract
The expression levels of miRNAs in cells or biological fluids are closely associated with the onset and progression of many diseases, making the detection of miRNAs in serum and plasma increasingly important. However, due to the low levels of miRNAs in biological fluids and the complexity of their surrounding environment, their analysis faces challenges related to accuracy and reproducibility. We developed a duplex-specific nuclease (DSN)-mediated detection method for the direct detection of miRNA-21 in real samples. This method eliminates the need for total RNA extraction from real samples using commercial kits, a key advantage over traditional methods requiring pre-treatment. As verified by performance evaluation, this method exhibits a linear range of 5.00 fmol·L^{-1} to 500 pmol·L^{-1} and a limit of detection (LOD) of 2.66 fmol·L^{-1} for miRNA-21. Direct detection of miRNA-21 in real samples yielded favorable results. These findings confirm that the method holds great application potential for the direct detection of miRNA-21 in real biological samples and exhibits promising prospects in clinical cancer diagnosis and drug screening.

Keywords MiRNA · Duplex-specific nuclease · Fluorescence detection · Hairpin probe

1 Introduction

MicroRNAs (miRNAs) are a class of endogenous non-coding single-stranded RNAs approximately 22 nucleotides in length. They interfere with intracellular messenger RNA (mRNA) through direct cleavage or indirect translational repression to regulate target gene expression, controlling biological processes such as cell proliferation, differentiation, and apoptosis (Bartel 2004; Dong et al. 2013; Lyu et al. 2024). Extensive research confirms that abnormal miRNAs expression is closely linked to numerous diseases, including cardiovascular diseases, diabetes, Alzheimer's disease (Swarbrick et al. 2019; Takousis et al. 2019), and cancers like breast cancer (Loh et al. 2019; Nurzadeh et al. 2021), gastric cancer (Kipkeeva et al. 2020), and cervical cancer (Aftab et al. 2021; Ren et al. 2025). Thus, miRNAs are promising biomarkers, and monitoring their expression in cells and blood is crucial for functional studies and early clinical diagnosis. However, their low in vivo abundance, high sequence similarity among homologous variants, and short length pose significant challenges for sensitive detection in real samples (Kilic et al. 2018; Mousazadeh et al. 2024), creating an urgent need for high-sensitivity and selective miRNA detection methods.

Traditional miRNA detection methods include microarray analysis (Clancy et al. 2017; Hu et al. 2018; Wu et al. 2013), northern blotting (Wang et al. 2010), and quantitative reverse transcription polymerase chain reaction (qRT-PCR) (Mariàngels and Rodicio 2013). Northern blotting is the most direct method, but low in sensitivity and is time-consuming, impractical for clinical studies requiring multiple miRNAs detections (Maroney et al. 2007). Microarray technology enables high-throughput analysis, but suffers from high cost, low sensitivity, and unvalidated detection accuracy (Sun and Sun 2020). The qRT-PCR offers a wide dynamic range, high sensitivity, good specificity, and simple operation, making it a common choice for low-abundance

✉ Chun-Guang Yang
yangcg@mail.neu.edu.cn

✉ Jin Li
lijin@symc.edu.cn

[1] Research Center for Analytical Sciences, Northeastern University, Shenyang 110819, P. R. China

[2] Shenyang Key Laboratory of Medical Molecular Theranostic Probes in School of Pharmacy, Shenyang Medical College, Shenyang 110034, P. R. China

Published online: 12 January 2026

miRNAs detection (Broseghini et al. 2025). Nevertheless, complex sample pretreatment is required due to the low abundance of miRNAs in complex samples (Kroh et al. 2010; Silva et al. 2025)—without it, results may be contaminated by genomic DNA. Additionally, the reliance on large, expensive instruments limits PCR applications in resource-constrained settings and clinical analysis.

In recent years, isothermal amplification technologies have gained attention for their high sensitivity and low instrument requirements, enabling rapid amplification at a constant temperature without PCR's thermal cycling (Deng et al. 2017; Yang et al. 2025). Among these, enzyme-mediated isothermal amplification is a promising PCR alternative, with duplex-specific nuclease (DSN) being a widely used substrate-specific enzyme for miRNAs amplification. DSN cleaves DNA in double-stranded DNA (dsDNA) and DNA-RNA hybrids without affecting single-stranded DNA (ssDNA) or RNA (Ma et al. 2021; Yuan et al. 2018), allowing target miRNA recycling and signal amplification (duplex-specific nuclease signal amplification, DSNSA) (Peng et al. 2018). Tian et al. (Tian et al. 2013) first established a DSN-mediated colorimetric detection method for miRNAs by designing a DNA probe with G-rich sequences at both ends that are released via hybridization and cleavage, binding to hemin to form a peroxidase-mimicking DNAzyme. This DNAzyme catalyzes the color reaction between $ABTS^{2-}$ and hydrogen peroxide, enabling label-free miRNA-141 detection within a linear range of 20 $pmol \cdot L^{-1}$ to 10 $nmol \cdot L^{-1}$. Despite its point-of-care (POC) advantage, colorimetric detection's low sensitivity limits sub-$pmol \cdot L^{-1}$ level miRNA detection. Zhang et al. (Zhang et al. 2018) improved this by combining DSN with catalytic hairpin assembly (CHA), achieving a detection limit of 9.2 $fmol \cdot L^{-1}$.

Electrochemical biosensors for miRNA detection are popular due to their low cost, ease of use, high portability, and simple construction. Jiao et al. (Jiao et al. 2020) designed a DSN-assisted target recycling strategy for $fmol \cdot L^{-1}$ level circular RNA (circRNA) detection, applied to human serum samples, showing clinical diagnosis potential. However, electrochemical biosensors face limitations such as limited biorecognition component stability and insufficient specific binding. DSN has also enhanced miRNA fluorescence detection. Wang et al. (Wang et al. 2020) proposed a magnetic nanobead-multicolor quantum dots assembly method for simultaneous detection of enterovirus 71-related miR-296 and miR-16, achieving $fmol \cdot L^{-1}$ level detection with single-base mismatch discrimination. Additionally, microfluidic fluorescence technology improved multiple biomarker detection as well as miRNA multiplex detection (Zhang et al. 2019; Ye et al. 2020) for its inherent advantages of miniaturization, low sample consumption, and high throughput. However, matrix interference remains a critical issue for real sample analysis, especially given the target miRNA's low abundance in clinical samples (Ma et al. 2021; Sun et al. 2025). Most methods require standard sample processing and RNA extraction to avoid interference from proteins and inorganic salts (Sun et al. 2021; Yang et al. 2021), narrowing their application scope and hindering clinical and on-site detection. Thus, there is an urgent need for simple and sensitive methods for direct real sample miRNA detection.

In this study, a simple and reliable direct detection method for miRNAs in real samples by combining DSN advantages with carboxylated polystyrene microspheres was developed. Capture probes (CP) were immobilized on the microsphere surface to specifically capture target miRNA-21, separating it from the complex matrix. After separation, miRNA-21 hybridized with hairpin-shaped detection probes (HP), restoring the quenched fluorescence, and the signal amplification was achieved via DSN-mediated cleavage. This method eliminates sample pretreatment and total RNA extraction, simplifying the workflow while ensuring high detection sensitivity.

Table 1 DNA and RNA sequences used in the experiment

Oligonucleotide	Sequences (5'→3')
FAM-DNA21	FAM-TAGCTTATCAGACTGATGTTGA
miRNA-21	UAG CUU AUC AGA CUG AUG UUG A
Hairpin probe (HP)	FAM-CGT CAA CAT CAG TCT GAT AAG CTA TTG ACG-BHQ1
Capture probe (CP)	NH_2-TTTTTTTTTTTCAACATCAGTCT GATAAGCTA
Sm-miRNA21	UAGCUUAUCAGACUGAUCUUGA
Tm-miRNA21	UAACUUAUCAGAAUGAUCUUGA
NC single strand	UUGUACUACACAAAAGUACUG

FAM 6-Carboxyfluorescein, *BHQ1* Black Hole Quencher Group, *DNA-21* mimic of miRNA-21, *SM-miRNA-21* miRNA sequence with a single base mismatch, *TM-miRNA-21* miRNA sequence with three base mismatches, *NC single strand* Irrelevant sequence of miRNA-21.

2 Experimental

2.1 Materials and reagents

DNA capture probes, DNA detection probes, synthetic miRNAs, and all other oligonucleotides were synthesized by Sangon Biotech Co., Ltd. (Shanghai, China). Duplex-specific nuclease (DSN) was purchased from Evrogen via Newborn Biotechnology Co., Ltd. (Shenzhen, China). The DNA and RNA sequences used in the experiment are shown in Table 1. DEPC-treated water (RNase-free) and ribonuclease inhibitors were obtained from Sangon Biotech Co., Ltd. (Shanghai, China). Solutions used for miRNA detection were prepared with DEPC-treated

water. Carboxylated polystyrene microspheres (100 μm in diameter) were purchased from Luminex Corporation. 1-Ethyl-3-(3-dimethylaminopropyl) carbodiimide (EDC), N-hydroxysulfosuccinimide (NHS), and 2-(N-morpholino) ethanesulfonic acid monohydrate (MES) were acquired from Aladdin Biochemical Technology Co., Ltd. (Shanghai, China). Imidazole and disodium ethylenediaminetetraacetate dihydrate ($Na_2EDTA \cdot 2\ H_2O$) were obtained from Sinopharm Chemical Reagent Co., Ltd. (Shanghai, China). Tris-HCl buffer was purchased from Regen Biotechnology Co., Ltd. (Beijing, China).

2.2 Preparation of buffer solution

Firstly, 50.0 mL of DEPC-treated water, 0.1017 g of $MgCl_2 \cdot 6\ H_2O$ (resulting in a final concentration of 5.00 mmol L^{-1}), and 0.0155 g of DTT (resulting in a final concentration of 1.00 mmol L^{-1}) were added sequentially into the 50.0 mL of 0.10 mol L^{-1} Tris-HCl buffer solution (pH 8.0). After being vigorously oscillated, the well-mixed buffer solution was further subjected to autoclaving and can then be used for the dilution, annealing, and hybridization of DNA.

To get a MES buffer solution with a pH of 6.0 and concentration of 50.00 mmol·L^{-1}, 0.9760 g of MES was dissolved in 70.0 mL of deionized water, then 10.0 mL of 1.00 mol·L^{-1} NaOH was added to the solution, and finally diluted to a final volume of 100.0 mL with deionized water.

2.3 Immobilization of capture probe on carboxylated microspheres

Carboxylated polystyrene (PS) microspheres were modified with 5'-end amino-modified DNA capture probes via EDC-NHS-mediated activation. The specific procedures were as follows. Firstly, 2.0 μL 25.0 mg·mL^{-1} carboxylated PS microspheres were washed three times with 200.0 μL of MES buffer. Subsequently, the carboxylated PS microspheres were transferred into 200.0 μL of 50.00 mmol L^{-1}MES buffer (pH = 6.0) containing 35.0 mg·mL^{-1} EDC and 55.0 mg·mL^{-1} NHS, followed by vigorous oscillation at 37 °C for 30 min to achieve activation. Secondly, 500 nmol·L^{-1} of 5'-end amino-modified DNA capture probes were added to the above solution, and the mixture was sufficiently oscillated at 37 °C for 1 h to allow the coupling reaction to proceed. Finally, uncoupled probes were removed by washing three times with Tris-HCl buffer. The resulting capture probe-immobilized PS microspheres (CP-PSs) were resuspended in 200.0 μL of Tris-HCl buffer and stored at 4 °C for subsequent use.

2.4 Detection of MiRNAs

Firstly, 5.0 μL of miRNA-21 standard solutions at different concentrations (with final concentrations of 5.00 fmol·L^{-1}, 50.0 fmol·L^{-1}, 500 fmol·L^{-1}, 5.00 pmol·L^{-1}, 50.0 pmol·L^{-1}, and 500 pmol·L^{-1}), 2.0 μL of hairpin probe (HP, hairpin-shaped detection probe, with a final concentration of 200 nmol·L^{-1}), 2.0 μL of RNase inhibitor (10.0 U·μL^{-1}), and 39.0 μL of Tris-HCl buffer were added separately to centrifuge tubes. Subsequently, the centrifuge tubes were placed in a constant-temperature incubator shaker maintained at 45 °C with a shaking speed of 170 rpm for a 1-hour reaction. After the reaction was completed, 2.0 μL of DSN (0.10 U·μL^{-1}) was added to each centrifuge tube. Finally, the centrifuge tubes were returned to the constant-temperature incubator shaker (45 °C, 170 rpm) for another 2-hour reaction. The entire reaction process was protected from light. Upon completion of the reaction, fluorescence detection was performed using a fluorescence spectrophotometer (F-4500, Hitachi Co., Ltd., Japan). The excitation wavelength was adjusted to 490 nm, and measurements were taken across the 510 to 700 nm spectrum. The maximum emission wavelength of FAM is chosen as 518 nm according to the fluorescence spectrum.

3 Results and discussion

3.1 Detection principle of MiRNAs

The miRNA-21 was selected as the target miRNA. A capture probe (CP, immobilized on carboxylated polystyrene (PS) microspheres as described in Section 2.3) and a hairpin probe (HP) were designed, where the HP contained a sequence fully complementary to miRNA-21. The 5'-end of the HP stem was conjugated with the fluorophore FAM, while the 3'-end was conjugated with the quencher BHQ1. To eliminate false positive signals, the stem region of HP was designed to contain 6 base pairs, ensuring the structural stability of the hairpin while precluding cleavage of HP by DSN (Vahabi et al. 2023; Hiniduma et al. 2025). As shown in Fig. 1, when HP is free in the Tris-HCl buffer, it adopts a closed hairpin conformation. Owing to its short stem, the hairpin structure fails to be recognized by DSN, resulting in the quenching of FAM fluorescence by BHQ1. In the presence of miRNA-21, HP hybridizes with miRNA-21 via sequence complementarity, inducing the hairpin structure to unfold. The spatial separation of FAM and BHQ1 leads to the recovery of FAM fluorescence. Simultaneously, DSN selectively cleaves the DNA strand within the HP-miRNA-21 DNA-RNA hybrid duplex, achieving complete spatial separation of FAM and BHQ1. The miRNA-21, remaining intact

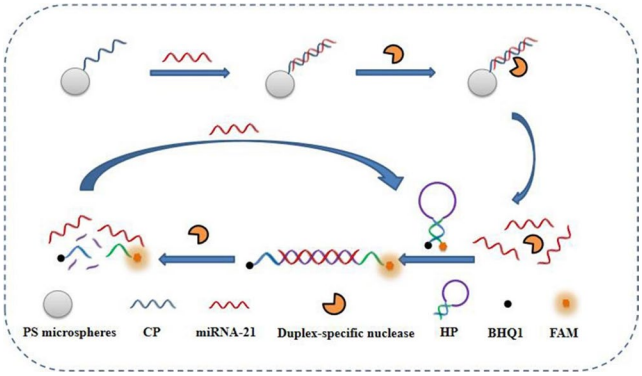

Fig. 1 Schematic illustration of the miRNA-21 detection principle based on duplex-specific nuclease

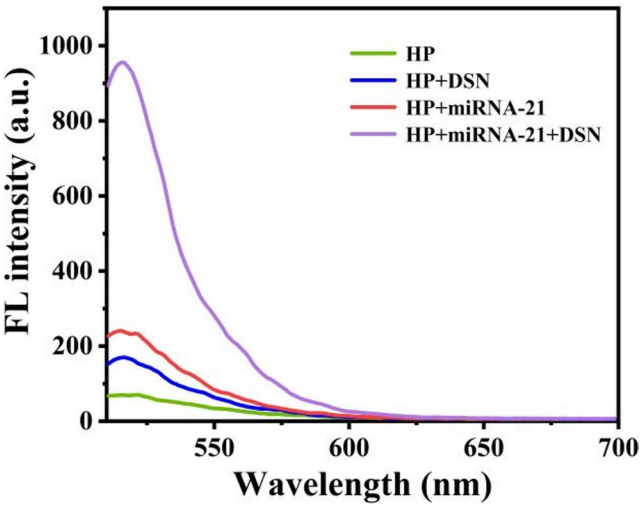

Fig. 2 Feasibility analysis of the DSN-mediated miRNA detection strategy. (Green: 200 nmol·L⁻¹ HP, Blue: 200 nmol·L⁻¹ HP+0.20 U DSN, Red: 200 nmol·L⁻¹ HP+10.0 nmol·L⁻¹ miRNA-21, Purple: 200 nmol·L⁻¹ HP+10.0 nmol·L⁻¹ miRNA-21+0.20 U DSN.)

after cleavage, is released and subsequently hybridizes with other free HP molecules to initiate a new round of cleavage. This cyclic process, featuring miRNA-21 recycling and continuous HP cleavage, culminates in substantial fluorescence signal amplification. The greater the number of recycling cycles miRNA-21 undergoes, the more HP molecules are cleaved, and the higher the detected fluorescence intensity.

To verify the feasibility of the proposed method, two sets of experiments were conducted. Primarily, we verified whether the CP immobilized on PS microspheres could capture the target strand. As shown in Fig. S1, the results demonstrated that the probes on the PS microspheres successfully captured the target in its presence. Furthermore, to validate the DSN-mediated miRNA-21 recycling process and the associated fluorescence amplification effect, fluorescence measurements were initially conducted using a 10.0 nmol·L⁻¹ miRNA-21 standard solution. As presented in Fig. 2, minimal fluorescence intensity was observed when only HP (200 nmol·L⁻¹) was present in the reaction system. In the DSN control group (200 nmol·L⁻¹ HP+0.20 U DSN), a slight increase in fluorescence intensity was detected. In the group containing HP and miRNA-21 (200 nmol·L⁻¹ HP+10.0 nmol·L⁻¹ miRNA-21), a modest fluorescence enhancement was observed, attributed to the specific hybridization between HP and miRNA-21. Notably, in the group with both miRNA-21 and DSN (200 nmol·L⁻¹ HP+10.0 nmol·L⁻¹ miRNA-21+0.20 U DSN), miRNA-21 was efficiently recycled via DSN-mediated cleavage, leading to a marked increase in fluorescence intensity. These results confirm that a low concentration of miRNA-21 can trigger the cleavage of a large quantity of HP molecules, thereby realizing fluorescence signal amplification. Collectively, these findings demonstrate the feasibility of the DSN-mediated miRNA detection strategy.

3.2 Optimization of experimental conditions

To evaluate the applicability of the DSN-mediated strategy for target miRNA detection, critical experimental conditions—specifically coupling buffer type and CP concentration—were optimized, as detailed below.

Three types of coupling buffers were compared, including 0.20 mol·L⁻¹ imidazole buffer, 0.01 mol·L⁻¹ PBS buffer, and 0.05 mol·L⁻¹ MES buffer. Detailed experimental procedures are provided in the supplementary material. The fluorescence intensity of CP-PSs treated with three different buffer solutions was quantified separately using a fluorescence microscope. As shown in Fig. 3, the highest coupling efficiency was observed in the MES buffer, which was thus selected as the optimal coupling buffer.

To maximize CP immobilization on PS microspheres, CP concentration was optimized. CP concentrations tested included 10.0 nmol·L^{-1}, 100 nmol·L^{-1}, 300 nmol·L^{-1}, 500 nmol·L^{-1}, 700 nmol·L^{-1}, and 1.00 μmol·L^{-1}. Following coupling, 1.0 μmol·L^{-1} FAM-modified DNA21 was added for hybridization at 37 °C for 1 h; unhybridized FAM-DNA21 was removed via centrifugation and washing, and microsphere fluorescence intensity was quantified. As presented in Fig. 4, fluorescence intensity increased with increasing CP concentration. A plateau was reached when the CP concentration reached 500 nmol·L^{-1}, indicating saturation of binding sites on PS microspheres. Therefore, 500 nmol·L^{-1} was chosen as the optimal CP concentration for subsequent experiments.

To ensure efficient cleavage and recycling, the reaction temperature was discussed in details. Because it affects the hybridization efficiency of nucleic acids and the cleavage efficiency of DSN, thereby influencing the detection results of the entire system. For nucleic acid hybridization, excessively high temperatures are unfavorable for nucleic acid

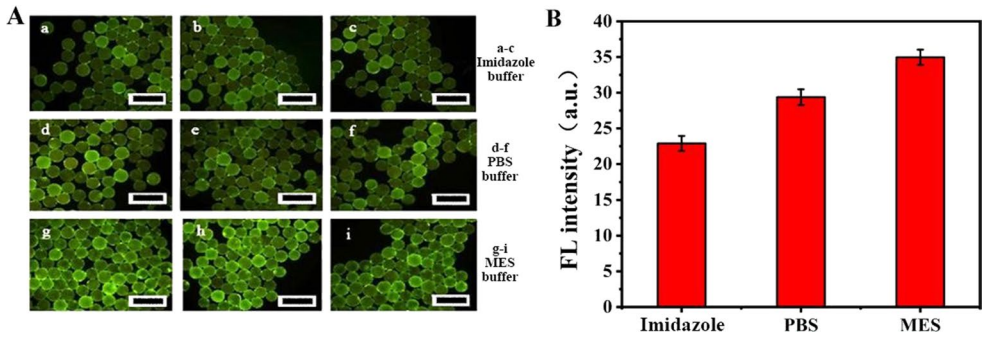

Fig. 3 Effect of coupling buffer on CP-PSs coupling efficiency. (**A**) Fluorescence microscopy images of CP-PSs microspheres in different buffers: (a-c) imidazole buffer; (d-f) PBS buffer; (g-i) MES buffer. Scale bar = 250 μm. (**B**) Quantitative analysis of fluorescence intensity for coupling efficiency in different buffers performed with the same fluorescence channel (FITC) and an exposure time of 100 ms

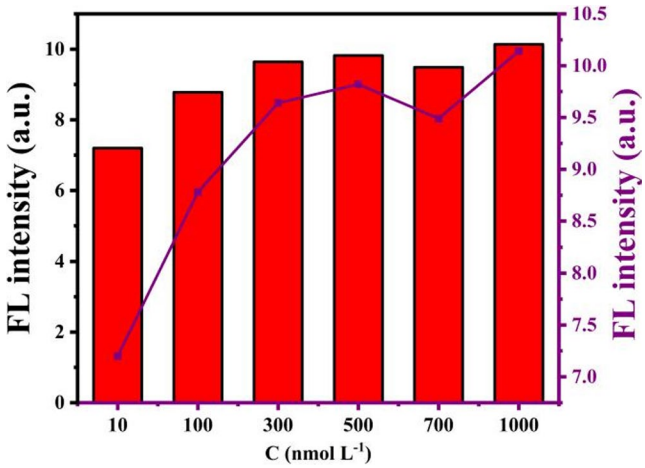

Fig. 4 Relationship between CP concentration and CP-PSs fluorescence intensity

renaturation; the optimal temperature is 25 °C lower than the Tm value. Since human body temperature is close to 37 °C, most nucleic acid hybridization reactions are conducted at 37 °C. The optimum temperature for DSN is 60 °C; however, its enzymatic activity decreases to 10% at 60 °C, and denaturation of dsDNA substrates may be one of the reasons for this sharp decline in enzymatic activity. To ensure both the activity of DSN and the smooth progression of nucleic acid hybridization, the reaction temperature was set at 45 °C.

According to the literatures (Peng et al. 2018; Zhang et al. 2018; Yin et al. 2012), the DSN-related reaction ranges from 40 min to 2 h, and the DSN dosage is about 0.2 U. In our work, to ensure the reaction proceeds sufficiently, the hybridization time was set to 1 h, the time for DSN-related cleavage cycle reaction was set to 2 h. As the dosage of DSN increases, the amplification efficiency improves; however, the background signal also increases simultaneously. Therefore, while ensuring the accuracy of experimental results, 0.2 U of DSN was added to each reaction centrifuge tube to save DSN dosage and control experimental costs.

3.3 Evaluation of the performance of DSN-mediated MiRNA detection

Under the aforementioned optimized conditions, the detection performance of the DSN-mediated miRNA-21 detection method was investigated. Specifically, the relationship between the concentration of miRNA-21 (ranging from 5.00 fmol·L^{-1} to 500 pmol·L^{-1}) and the amplified fluorescence signal was determined.

When the concentration of the analyte (miRNA-21) was 0 (i.e., using a target-free blank as the background), the measured fluorescence intensity at 518 nm was defined as F_0. The fluorescence intensity at 518 nm obtained after adding miRNA-21 at different concentrations was defined as F. The detection performance of the method was evaluated using the relative fluorescence intensity, calculated as the difference between the post-reaction fluorescence and the background fluorescence ($F - F_0$). As the fluorescence spectrum represents the relative fluorescence intensity detected by the detector, not the inherent property of the analyte, the intensity values F, F_0, and (F-F_0) are dimensionless and have no physical units in this work. But it has no impact on the quantitative measurement and result discussion.

As shown in Fig. 5, when the concentration of miRNA-21 varied from 5.00 fmol·L^{-1} to 500 pmol·L^{-1}, the value $(F - F_0)$ exhibited a good linear relationship with the logarithm of the miRNA-21 concentration. This linear relationship followed the regression equation $\mathbf{y = 42.00\ lg\ x + 175.53}$ ($\mathbf{R^2 = 0.9987}$), where x denotes the concentration of miRNA-21 (pmol·L^{-1}) and y denotes the difference of the relative fluorescence intensity $(F - F_0)$, and each measurement was repeated three times.

The limit of detection (LOD) of this method for miRNA-21 was calculated using the formula $\mathbf{LOD = 3\sigma/slope}$, where σ represents the standard deviation of the fluorescence intensity of the blank sample measured in triplicate, and slope refers to the slope of the linear regression equation. The resulting LOD was 2.66 fmol·L^{-1}.

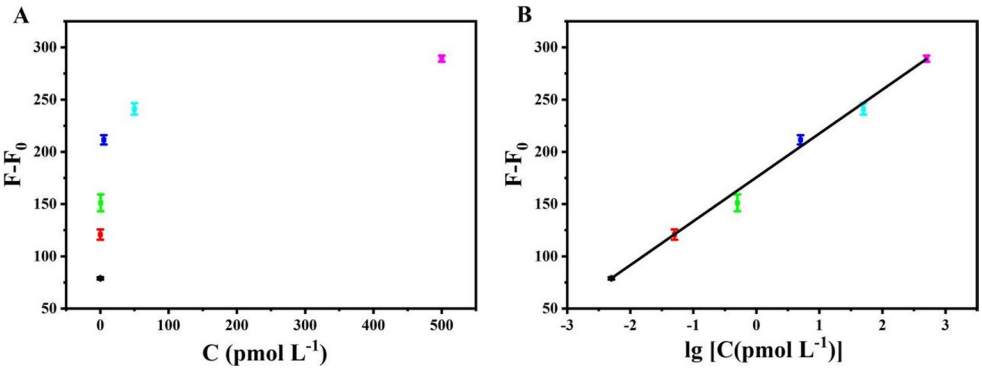

Fig. 5 Calibration curve of F-F_0 versus miRNA-21 concentration: (**A**) Difference in fluorescence intensity (F-F_0) versus miRNA-21 concentration (pmol L^{-1}); (**B**) Difference in fluorescence intensity (F-F_0) versus lg [miRNA-21 concentration (pmol L^{-1})]. The error bars indicate the standard deviation calculated from three separate experiments

Table 2 Comparison of this method with other detection methods

Target	Amplification Strategy	Detection Method	Linear Range	LOD	Detection Duration	Ref.
miRNA-21	DSNSA	Fluorescence	0–80 nmol·L^{-1}	500 pmol·L^{-1}	41 min	(Cai et al. 2018)
let-7a	Branched RCA	Fluorescence	100 fmol·L^{-1}–10 nmol·L^{-1}	58 fmol·L^{-1}	>4 h	(Wang et al. 2015)
miRNA-21	MCE-LIF	Fluorescence	10 fmol·L^{-1}–1 nmol·L^{-1}	1.0 fmol·L^{-1}	4 h	(Chen et al. 2022)
miRNA-21	LICA	Fluorescence	0–5 pmol·L^{-1}	221 fmol·L^{-1}	4.5 h	(Zhang et al. 2026)
miRNA-21	RCA	Fluorescence	5–25 pmol·L^{-1}	0.49 pmol·L^{-1}	not mentioned	(Johne et al. 2009)
miRNA-21	DSNSA	Mass Spectrometry	0.2 pmol·L^{-1}–0.5 nmol·L^{-1}	60 fmol·L^{-1}	1 h	(Pang et al. 2016)
circRNA	DSNSA	Electrochemistry	10 fmol·L^{-1}–100 pmol·L^{-1}	3.47 fmol·L^{-1}	3.6 h	(Yang et al. 2019)
miRNA-21	DSN-Mediated Amplification	Fluorescence	5.00 fmol·L^{-1}–500 pmol·L^{-1}	2.66 fmol·L^{-1}	3 h	This Work

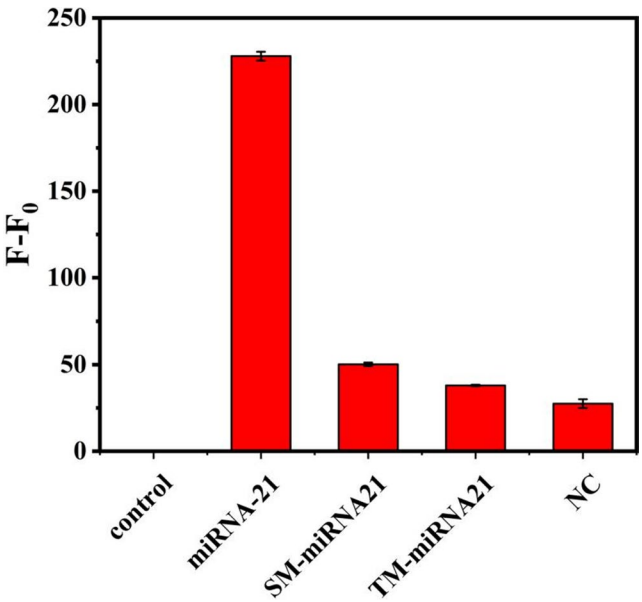

Fig. 6 The specificity of the method for DSN-mediated miRNA detection. The error bars indicate the standard deviation calculated from three separate experiments

Table 2. Summarizes several other reported miRNA detection methods. In comparison, the DSN-mediated method developed in this study exhibits superior sensitivity in fluorescence methods and is comparable to that of the electrochemistry method.

3.4 Specificity of the method for DSN-mediated MiRNA detection

Given the short sequence length of miRNAs and high sequence homology among their family members, the evaluation of selectivity towards the target is a critical performance metric for miRNA detection methods. A miRNA detection method with excellent specificity should be capable of distinguishing between homologous miRNAs and coexisting base-mismatched miRNAs, enabling the selective detection of the target miRNA in complex samples.

To verify the specificity of the method proposed in this work, non-complementary (NC) single-stranded RNA, single-base mismatched miRNA-21 (SM-miRNA-21), and three-base mismatched miRNA-21 (TM-miRNA-21) were used as non-complementary RNA controls to evaluate the method's selectivity. As shown in Fig. 6, a strong fluorescence signal was only observed in the reaction system containing the target miRNA-21, while the other control groups exhibited weak fluorescence signals. Thus, the proposed method can distinguish single-base mismatched miRNAs coexisting with the target miRNA, demonstrating that the system has excellent specificity and holds great application potential in the field of single-nucleotide polymorphism (SNP) analysis.

Table 3 Spike-and-recovery experiment of miRNA-21 in human serum samples ($n=3$)

Sample	Spiked concentration ($pmol \cdot L^{-1}$)	Detected concentration ($pmol \cdot L^{-1}$)	Recovery (%)	RSD(%)
1	5.00	6.60	132	3.5
2	50.0	62.0	124	4.3
3	500	568	113	0.63

3.5 Application of the DSN-mediated MiRNA detection method in real sample assay

To verify the accuracy of the DSN-mediated direct miRNA-21 detection method for real biological sample analysis, serum from healthy individuals was selected as the test sample. Spike-and-recovery experiments for the target miRNA-21 at concentrations of 5 pM, 50 pM, and 500 pM were conducted in a 10-fold diluted serum matrix. As shown in Table 3, the calculated relative standard deviations (RSDs) ranged from 0.63% to 4.3%. Although the recovery rates were all above 100%, which may be due to endogenous miRNA-21 in the serum samples contributing to the total signal, these results still indicated that other biomolecules in human serum do not significantly interfere with the detection of target miRNA-21.

To further evaluate the feasibility of the DSN-mediated method for direct detection of target miRNA-21 in real biological samples, human serum and tumor cell lysates were selected as the test samples. Target miRNA-21 in these two sample types was detected directly without prior total RNA extraction. First, miRNA-21 was detected in serum samples from breast cancer patients, pancreatic cancer patients, and healthy individuals, respectively. As shown in Fig. 7 (A), the expression levels of miRNA-21 in serum from breast cancer and pancreatic cancer patients were significantly higher than those in serum from healthy individuals. This observation is consistent with previous reports (Itani et al. 2021; Smolarz et al. 2021).

Subsequently, miRNA-21 was detected in the human breast cancer cell line (MCF-7) and the human cervical cancer cell line (HeLa). The detection results for the two cell lysates are presented in Fig. 7 (B); the fluorescence intensity of the MCF-7 sample was slightly higher than that of the HeLa sample, which is also consistent with previous literature (Krol et al. 2010).

In conclusion, based on all experimental results of this study, the proposed method is demonstrated to have considerable reliability for miRNA-21 detection and holds potential application value in the diagnosis and treatment of miRNA-21-related diseases.

4 Conclusions

In this study, a direct detection method for target miRNA in real samples was developed using DSN. DSN is a promising bioanalytical tool, as it cleaves DNA within DNA-RNA duplexes while preserving the integrity of RNA strands. This unique property allows the target miRNA to remain continuously involved in the reaction, enabling cyclic signal amplification. Benefiting from DSN-mediated cyclic signal amplification, the method exhibits significantly improved detection sensitivity. Moreover, leveraging the characteristics of hairpin-shaped detection probes and substrate specificity of DSN, the method can distinguish highly similar miRNA sequences with single-base differences, confirming its excellent selectivity. Additionally, by using capture probes immobilized on polystyrene microspheres, the method enables direct detection of target miRNAs in complex real samples without any pre-treatment steps, thereby simplifying the overall detection procedure. Furthermore, multiplex miRNA detection can be easily achieved by designing sequence-matched CP and HP for different targets. Experimental results demonstrate that for miRNA-21 detection, the method has a linear range of 5.00 $fmol \cdot L^{-1}$ to 500 $pmol \cdot L^{-1}$ and LOD of 2.66 $fmol \cdot L^{-1}$. The method was successfully applied to detect miRNA-21 in serum from healthy individuals, breast cancer patients, and pancreatic cancer patients, as well as in lysates of two tumor cell lines, MCF-7 and HeLa. And the method also yielded satisfactory outcomes in spike-and-recovery experiments with human serum. Thus, the DSN-mediated method holds great application potential for the direct detection of miRNA-21 in real

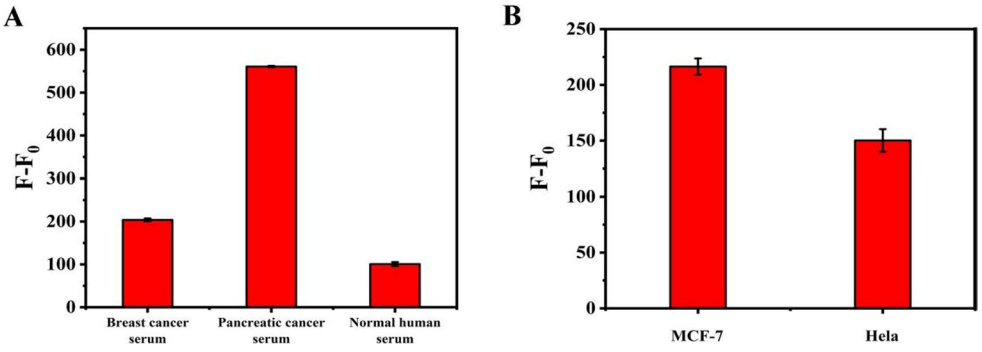

Fig. 7 Detection of target miRNA-21 in real samples. (**A**) Detection results of miRNA-21 in serum samples (normal human serum, pancreatic cancer serum, breast cancer serum). (**B**) Detection results of miRNA-21 in cell lysates (MCF-7, HeLa)

biological samples and exhibits promising prospects in clinical cancer diagnosis and drug screening. Since the recognition of target sequences in this work is achieved through Watson–Crick base pairing, the proposed method can be extended to other target miRNAs by simply redesigning the capture and hairpin probes according to the sequence of the new target miRNA. In addition, in order to facilitate its application in point-of-care testing (POCT), replacing with higher-performance fluorescent dyes to obtain stronger fluorescent signals in a shorter time, as well as organically integrating the detection system with a microfluidic platform to reduce reaction time, will be our subsequent plans and attempts to break through the limitation of detection duration.

Supplementary Information The online version contains supplementary material available at https://doi.org/10.1007/s10544-025-00789-4.

Acknowledgements The authors appreciate financial support from the Natural Science Foundation Joint Fund of Liaoning Province (2023-BSBA-299), Basic Scientific Research Program of the Educational Department of Liaoning Province (LJ212510164015), and Shenyang Medical College Project (20249083). Special thanks are due to the instrumental and data analysis from the Research Center for Analytical Sciences, Northeastern University.

Author contributions Chun-Guang Yang: Investigation, Conceptualization, Data curation, Writing - Original Draft, Writing - review & editing.Yi Han: Conceptualization, Validation, Methodology, Data curation, Writing-Original Draft.Jing-Jing Zhang: Investigation, Data curation.Li-Wen Xu: Investigation, Validation.Jin Li: Funding acquisition, Project administration, Resources, Supervision, Writing – review & editing.

Data availability No datasets were generated or analysed during the current study.

Declarations

Ethical statement All serum samples were analyzed fresh or flash-frozen and stored at -80 ℃ for future analysis. The serum samples from healthy humans were collected from volunteers. The serum samples from cancer patients were collected from the First Affiliated Hospital of China Medical University. This study was approved by the Biological and Medical Ethics Committee of Northeastern University (approval: EC-2023B022).

Competing interests The authors declare no competing interests.

References

B. Smolarz, A. Durczynski, H. Romanowicz et al., The role of MicroRNA in pancreatic cancer. Biomedicines. **9**(10), 1322 (2021)

B.C. Yin, Y.Q. Liu, B.C. Ye, One-step, multiplexed fluorescence detection of microRNAs based on duplex-specific nuclease signal amplification. J. Am. Chem. Soc. **134**, 5064–5067 (2012)

B.J. Cai, S. Guo, Y. Li, MoS_2-based sensor for the detection of MiRNA in serum samples related to breast cancer. Anal. Methods. **10**, 230–236 (2018)

D. Wu, Y. Hu, S. Tong et al., The use of miRNA microarrays for the analysis of cancer samples with global miRNA decrease. RNA **19**, 876–888 (2013)

D.P. Bartel, MicroRNAs: genomics, biogenesis, mechanism, and function. Cell. **116**(2), 281–297 (2004)

E. Broseghini, B. Fontana, G. Durante et al., Quantification of tissue and Circulating MicroRNAs by droplet digital PCR. Methods Mol. Biol. **2969**, 195–233 (2025)

E. Clancy, M. Burke, V. Arabkari et al., Amplification-free detection of MicroRNAs via a rapid microarray-based sandwich assay. Anal. Bioanal Chem. **409**, 3497–3505 (2017)

E.M. Kroh, R.K. Parkin, P.S. Mitchell et al., Analysis of circulating microrna biomarkers in plasma and serum using quantitative reverse transcription-PCR (qRT-PCR). Methods **50**(4), 298–301 (2010)

F. Kipkeeva, T. Muzaffarova, A. Korotaeva et al., Microrna in gastric cancer development: mechanisms and biomarkers. Diagnostics **10**(11), 891 (2020)

G.M. Ma, L.W. Huo, Y.X. Tong et al., Label-free and sensitive mirna detection based on turn-on fluorescence of DNA-templated silver nanoclusters coupled with duplex-specific nuclease-assisted signal amplification. Mikrochim. Acta **188**, 355 (2021)

H.F. Dong, J.P. Lei, L. Ding et al., MicroRNA: function, detection, and bioanalysis. Chem. Rev. **113**(8), 6207–6233 (2013)

H.M. Zhang, K.Y. Wang, S.J. Bu et al., Colorimetric detection of microRNA based on DNAzyme and nuclease-assisted catalytic hairpin assembly signal amplification. Mol. Cell. Probes **38**, 13–18 (2018)

H.Y. Loh, B.P. Norman, K.S. Lai et al., The regulatory role of MicroRNAs in breast cancer. Int. J. Mol. Sci. **20**(19), 4940 (2019)

J. Hu, X. Yue, J.Z. Liu et al., Construction of an MiRNA–gene regulatory network in colorectal cancer through integrated analysis of mRNA and MiRNA microarrays. Mol. Med. Rep. **18**(6), 5109–5116 (2018)

J. Jiao, C. Li, L.M. Ning et al., Electrochemical detection of circrnas based on the combination of back-splice junction and duplex-specific nuclease. Sens. Actuat B-Chem. **302**, 127166 (2020)

J. Krol, I. Loedige, W. Filipowicz, The widespread regulation of microrna biogenesis, function and decay. Nat. Rev. Genet. **11**, 597–610 (2010)

J.D. Sun, X.L. Sun, Recent advances in the construction of DNA nanostructure with signal amplification and ratiometric response for miRNA sensing and imaging. TrAC Trends Anal. Chem. **127**, 115900 (2020)

J.J. Wang, C. Zheng, Y.Z. Jiang et al., One-step monitoring of multiple enterovirus 71 infection-related MicroRNAs using core–satellite structure of magnetic nanobeads and multicolor quantum Dots. Anal. Chem. **92**(1), 830–837 (2020)

J.P. Yang, J. Chen, L. Xia et al., Recent progress on biosensors for detection of Circulating MiRNA biomarkers. Talanta. **294**, 128219 (2025)

K. Hiniduma, T.D. Silva, R. Canete et al., ECL-CRISPR array for multiplexed detection of MiRNAs. Biosens. Bioelectron. **289**, 117855 (2025)

L.D. Wang, R.J. Deng, J.H. Li, Target-fueled DNA walker for highly selective miRNA detection. Chem. Sci. **6**, 6777–6782 (2015)

M. Aftab, S.S. Poojary, V. Seshan et al., Urine MiRNA signature as a potential non-invasive diagnostic and prognostic biomarker in cervical cancer. Sci. Rep. **11**, 10323 (2021)

M. Mousazadeh, M. Daneshpour, S.R. Tafti et al., Nanomaterials in electrochemical nanobiosensors of mirnas. Nanoscale **16**, 4974–5013 (2024)

M. Nurzadeh, M. Naemi, S.S. Hasani, A comprehensive review on oncogenic miRNAs in breast cancer. J. Genet. **100**, 15 (2021)
M. Vahabi, B. Dehni, I. Antomás et al., Targeting miRNA and using miRNA as potential therapeutic options to bypass resistance in pancreatic ductal adenocarcinoma. Cancer Metastasis Rev. **42**, 725–740 (2023)
M.M. Itani, F.J. Nassar, A.H. Tfayli et al., A signature of four Circulating MicroRNAs as potential biomarkers for diagnosing early-stage breast cancer. Int. J. Mol. Sci. **22**(11), 6121 (2021)
P. Takousis, A. Sadlon, J. Schulz et al., Differential expression of MicroRNAs in alzheimer's disease brain, blood, and cerebrospinal fluid. Alzheimer's Dement. **15**(11), 1468–1477 (2019)
P.A. Maroney, S. Chamnongpol, F. Souret et al., A rapid, quantitative assay for direct detection of micrornas and other small RNAs using splinted ligation. RNA **13**, 930–936 (2007)
P.I.T. De Silva, K. Hiniduma, R. Canete et al., Multiplexed CRISPR assay for amplification-free detection of miRNAs. Biosensors **15**(6), 346 (2025)
P.-S. de Mariàngels, M.C. Rodicio, Detection methods for MicroRNAs in clinic practice. Clin. Biochem. **46**(10–11), 869–878 (2013)
R. Johne, H. Muller, A. Rector et al., Rolling-circle amplification of viral DNA genomes using phi29 polymerase. Trends Microbiol. **17**(5), 205–211 (2009)
R.J. Deng, K.X. Zhang, J.H. Li, Isothermal amplification for microRNA detection: from the test tube to the cell. Acc. Chem. Res. **50**(4), 1059–1068 (2017)
S. Swarbrick, N. Wragg, S. Ghosh et al., Systematic review of miRNA as biomarkers in Alzheimer's disease. Mol. Neurobiol. **56**, 6156–6167 (2019)
S.Y. Chen, J.J. Zhao, I.Y. Sakharov et al., An ultrasensitive multivariate signal amplification strategy based on microchip platform tailored for simultaneous quantification of multiple MicroRNAs in single cell. Biosens. Bioelectron. **203**, 114053 (2022)
S.Z. Zhang, R.Z. Liu, R.K. Liu et al., Ultrasensitive miRNA-21 detection via catalytic hairpin assembly-enhanced light-initiated chemiluminescence for early cancer diagnosis. Talanta **298**, 128913 (2026)
T. Kilic, A. Erdem, M. Ozsoz et al., MicroRNA biosensors: opportunities and challenges among conventional and commercially available techniques. Biosens. Bioelectron. **99**, 525–546 (2018)
T. Tian, H. Xiao, Z.G. Zhang et al., Sensitive and convenient detection of MicroRNAs based on cascade amplification by catalytic dnazymes. Chem. Eur. J. **19**(1), 92–95 (2013)
X.Y. Lyu, H.Y. Wu, M.Z. Xu et al., A bioswitchable MiRNA delivery system: tetrahedral framework DNA-based MiRNA delivery system for applications in wound healing. ACS Appl. Mater. Interfaces. **16**(26), 33192–33204 (2024)
W.P. Peng, Q. Zhao, J.F. Piao et al., Ultra-sensitive detection of microRNA-21 based on duplex-specific nuclease-assisted target recycling and horseradish peroxidase cascading signal amplification. Sens. Actuators B Chem. **263**, 289–297 (2018)
W.Q. Ye, Y.X. Wei, Y.Z. Zhang, C.G. Yang, Z.R. Xu, Multiplexed detection of micro-RNAs based on microfluidic multi-color fluorescence droplets. Anal. Bioanal. Chem. **412**, 647–655 (2020)
X. Ren, G. Liu, J. Zhou, Nuclear-activating mirnas: unveiling the intricacies of subcellular miRNA function and regulation in cancer and immunity disease. Cancer Cell. Int. **25**, 147 (2025)
X.S. Wang, Y.G. Tong, S.H. Wang, Rapid and accurate detection of plant miRNAs by liquid northern hybridization. Int. J. Mol. Sci. **11**(9), 3138–3148 (2010)
Y.F. Pang, C.W. Wang, J. Wang et al., Fe_3O_4@ ag magnetic nanoparticles for MicroRNA capture and duplex-specific nuclease signal amplification based SERS detection in cancer cells. Biosens. Bioelectron. **79**, 574–580 (2016)
Y.H. Yuan, B.Z. Chi, S.H. Wen et al., Ratiometric electrochemical assay for sensitive detecting MicroRNA based on dual-amplification mechanism of duplex-specific nuclease and hybridization chain reaction. Biosens. Bioelectron. **102**, 211–216 (2018)
Y.J. Sun, C.C. Wang, L. Tang et al., Magnetic-enhanced fluorescence sensing of tumor MiRNA by combination of MNPs@PDA with duplex specific nuclease. RSC Adv. **11**(5), 2968–2975 (2021)
Y.M. Yang, S.W. Liu, X.F. Cui et al., Sensitive detection of MiRNA based on enzyme-propelled multiple photoinduced electron transfer strategy. Mikrochim Acta. **188**, 219 (2021)
Y.Y. Sun, Y.L. Sun, Y.F. Peng et al., High sensitivity and specificity analysis of multiple miRNAs. Anal. Chim. Acta **1369**, 344341 (2025)
Y.Z. Zhang, W.Q. Ye, C.G. Yang, Z.R. Xu, Simultaneous quantitative detection of multiple tumor markers in microfluidic nanoliter-volume droplets. Talanta. **205**, 120096 (2019)
Z.Q. Yang, L. Qin, D.T. Yang et al., Signal amplification method for miR-205 assay through combining graphene oxide with duplex-specific nuclease. RSC Adv. **9**, 27341–27346 (2019)